ISSN 2278-2540 | DOI: 10.51583/IJLTEMAS | Volume XV, Issue VI, June 2026

Development of stimuli-responsive polymeric hydrogels and their applications

[1]Dr. Pronob Gogoi and [2]Dr. Monalisha Boruah*

[1]Department of Chemistry, Diphu Government College, Diphu, Karbi Anglong, Assam, 782462

[2]Dimension Academy Senior Secondary School, Harigaon, Tezpur, Sonitpur, Assam, 784001

DOI: https://doi.org/10.51583/IJLTEMAS.2026.150600232

Received: 10 July 2026; Accepted: 15 July 2026; Published: 28 July 2026

ABSTRACT

Electro-responsive nanocomposite hydrogels based on gelatin, partially neutralized acrylic acid (PAAc), and acid-functionalized multiwalled carbon nanotubes (MWCNT-COOH) were developed and evaluated as potential smart drug delivery systems. The successful functionalization of pristine MWCNTs was confirmed by the shift in characteristic X-ray diffraction (XRD) peaks, while the presence of MWCNT-COOH peaks in the nanocomposite hydrogel verified their effective incorporation into the polymer matrix. Scanning electron microscopy (SEM) revealed distinct morphological changes following acid functionalization and demonstrated the uniform dispersion of MWCNT-COOH within the hydrogel network, resulting in a smooth and homogeneous surface. Swelling studies showed that increasing MWCNT-COOH content reduced the swelling percentage in the absence of an electric field, whereas the application of a 10 V electric field significantly enhanced swelling, confirming the electro-responsive nature of the hydrogels. In vitro hemolysis assays indicated excellent blood compatibility, highlighting their suitability for biomedical applications. The electro-responsive release of vitamin B_{12} was strongly influenced by the ionic strength of the release medium, applied voltage, and MWCNT-COOH concentration. Furthermore, drug release behavior was systematically optimized using response surface methodology based on a central composite design. Overall, the developed Gelatin-g-PAAc/MWCNT-COOH nanocomposite hydrogels exhibit favorable structural, swelling, biocompatible, and electro-responsive characteristics, making them promising candidates for the design of advanced electrically controlled drug delivery systems.

Keywords: Nanocomposite, hydrogel, electro-responsive, drug delivery, MWCNTs.

INTRODUCTION

In recent times, stimuli-responsive polymeric hydrogels constitute a new generation of biomaterials for a wide range of applications such as drug delivery, tissue engineering, bioseparation, sensors, actuators etc.[1-3] Despite many advantages of using conventional hydrogels, their applications are often limited due to their poor mechanical and some restricted response properties.[4] So, attention has been given to improve the properties of a hydrogel such as mechanical strength, thermal properties, response to a stimuli etc. In the current scenario of drug delivery technologies, hydrogels have emerged an irreplaceable space because of their special three dimensional network structure which can effectively provide a matrix for the entrapment of drugs.[5]

It is obvious that the precise controls over the drug quantity and the release rate are required in order to optimize the drug release. Now- a -days, pulsatile drug release devices are extensively developed which releases drug at a predetermined time or in pulses of a predetermined sequence. These systems have been shown to alter their rate of drug delivery in response to various stimuli.[6] Therefore, stimuli-responsive polymeric hydrogels have been profoundly employed as intelligent drug delivery systems. Amongst various stimuli-responsive drug delivery systems, electro-responsive hydrogels which carry free cations or anions are fascinating materials for the design of electrically modulated drug-delivery systems.[7] The advantages of an electric field as an external stimulus are accessibility of equipment, which imparts precise control with respect to the magnitude of the current, duration of electric pulses, interval between pulses[8] etc. Electro-responsive behavior of the hydrogels

ISSN 2278-2540 | DOI: 10.51583/IJLTEMAS | Volume XV, Issue VI, June 2026

can be significantly improved by the successful incorporation of different conducting polymers such as polyaniline,[9] polypyrrol etc. or different carbon conducting fillers such as graphite,[10, 11] carbon fibers,[12] carbon black[13] and carbon nanotubes[14] into the hydrogel matrix.

Both single-walled (SWCNT) and multi-wall (MWCNT) carbon nanotubes are promising nanomaterials with great potential in the field of nanomedicine for both therapeutic and diagnostic applications.[15] They have also been proved to be advanced multi-functional fillers in polymer-based nanocomposites.[16] But, incorporation of CNTs into different polymeric systems becomes a technical challenge due to their poor dispersibility in water or organic solvents.[17,18] So, this problem has been removed by chemical functionalization, in which some strong oxidants are used to generate carboxyl group on the surface of CNTs.[19] Moreover, it has been already reported that the biocompatibility of carbon nanotubes can be enhanced by the surface functionalization and introduction of hydrophilic moieties to avoid unwanted cytotoxic responses and risks for carcinogenesis.[20] Gelatin is a low cost material and has been extensively studied to be used as a biomaterial like artificial skin, bone grafts, and scaffolds for tissue engineering[21-24] etc. Its physicochemical properties can be suitably modulated by developing composites or nanocomposites through the introduction of some reinforcing fillers into its structure.[25]

Various approaches have been demonstrated in the literature describing the preparation of electro-responsive drug delivery systems using hydrogels. Kulkarni et al. developed polyacrylamide-g-alginate based electrically responsive hydrogel for drug delivery application. A pulsatile pattern of drug permeation was observed as electric stimulus was switched on and off.[26] Banga et al. synthesized polyacrylamide hydrogels and demonstrated the feasibility of the prepared hydrogels in iontophoretic release and transdermal delivery of three model peptides, insulin, calcitonin and vasopressin under an applied electric field. It was observed that the release of drug from a hydrogel matrix under action of electric field strength was more than the release in the absence of electric field and the release can be precisely controlled.[27] Kim et al. investigated the electrically modulated delivery of ionic drug cefazoline from electro-active Poly(vinyl alcohol)/Poly(acrylic Acid) IPN hydrogels. The rapid release behaviors of cefazoline were observed when an electric stimulus was at "ON" state, whereas they showed relatively slow release during the "OFF" state.[28] Tanaka et al. demonstrated that the partially hydrolyzed polyacrylamide gel undergoes phase transition upon application of an electric field, and collapsed if the gel was placed in a solvent such as 50% acetone-water binary mixture.[29]

Modern optimization techniques using experimental designs are important assistance to the formulator, as they help in developing the best possible formulation under a given set of conditions, consequently saving considerable time, money and developmental effort.[30,31] Moreover, these systematic techniques are known to provide a depth of understanding and ability to explore and defend the ranges for varied formulation and processing factors. In this regard, Central composite design (CCD) has been frequently employed for the optimization of controlled drug delivery systems.[32] The advantages of experimental design method over classical experimental approach are, the reduction in the number of trials, ability to cover a large number of factors, the detection of interactions between factors, detection of optimum reaction condition, a higher precision of the response data and the empirical modeling of the data.[33] Statistical methods, such as response surface methodology are used in developing and optimizing polymeric systems for a wide range of applications.[34] For example, Li et al. performed the optimization of sustained release matrix tablet of metoprolol succinate using central composite design. After investigating the effects of various parameters on drug release, a 2-factor, 5-level central composite design was employed. Response surfaces were also established to obtain the matrix ranges and the main factors affecting four responses. They predicted that this matrix combination can be used as a good alternative to the commercially pellet technology, which was complicated, time-consuming and energy-intensive.[35]

Observing the significant applications of electro-responsive nanocomposite hydrogel, the present chapter involves the development of a pH and electro-responsive nanocomposite hydrogel based on Gelatin-g-poly(acrylic acid) and acid functionalized multiwall-carbon nanotubes. Physical characteristics such as molecular structure and surface morphology of the prepared hydrogels were investigated thoroughly. We examined the release behavior of vitamin B_{12} at different applied voltages and ionic strength of the release media. Also, the effect of time, MWCNT-COOH content and applied voltage on electro-responsive drug release behavior was studied by response surface analysis. Vitamin B_{12} is a water-soluble vitamin with a key role in the

ISSN 2278-2540 | DOI: 10.51583/IJLTEMAS | Volume XV, Issue VI, June 2026

normal functioning of the nervous system and for the formation of blood.[36] Therefore, vitamin B_{12} is chosen as a model drug.

Experimental

Materials

Acrylic acid monomer (Aldrich) was distilled under reduced pressure prior to use. Gelatin A (300 Bloom), ammonium persulfate (initiator), methylene bis-acrylamide (MBA) as a crosslinking agent and N, N, N', N'-tetramethylethylene diamine were supplied by Aldrich (A.R. grade). Multiwall carbon nanotubes (MWCNTs) were supplied from Shenzhen Nanotech Port Co., Ltd., China. Nitric acid, sodium hydroxide and ethanol (A. R grade) were purchased from Merck, Mumbai. Vitamin B_{12} ($C_{63}H_{88}CoN_{14}O_{14}P$) was purchased from Merck, Mumbai (M.W= 1355.4 g/mol).

Preparation of Gelatin-g-poly(acrylic acid)/MWCNTs nanocomposite hydrogel

Acid treatment of MWCNT

Functionalization of CNTs with different chemical groups is generally used to enhance their dispersibility in water and the mostly used technique for this purpose is the oxidization with strong oxidants to generate carboxyl group on the surface of CNTs. In this case, the carboxylic acid functionalized MWCNTs were prepared according to the earlier described method.[37,38] 60 mg of MWCNTs were added to a round-bottom flask containing 50 ml of 60% HNO_3 aqueous solution. The mixture was refluxed for 6 hrs and then cooled to room temperature. The mixture was diluted with 500 ml of deionized water and then collected by low speed centrifugation. The obtained product was washed with deionized water until the pH of the filtrate reached 7 and was dried under vacuum for 24 hrs at 80 ^oC.

Preparation of Gelatin-g-PAAc/MWCNTs nanocomposite hydrogel

Gelatin-g-poly(acrylic acid) /MWCNT-COOH nanocomposite hydrogels were prepared by free radical polymerization in distilled water. 2 g of gelatin was dissolved in 30 ml of distilled water at 60^oC and partially neutralized (60%) acrylic acid monomer was added to this solution. Also, MWCNT-COOH (0.1-0.6 wt%) was added to gelatin-acrylic acid mixture and dispersed under the ultrasonic vibration for 30 min. Subsequently, methylene bis-acrylamide (0.05-0.25 wt%), ammonium persulfate (1.0 wt%) and TEMED (0.05 ml) were added to the mixture under continuous stirring. Nitrogen was used to remove dissolved oxygen from the reactive solution. The reactive solution was first prepolymerizd at 60^oC for 1 hr under stirring, and then poured into a petri dish quickly. The post polymerization was carried out at 70^oC for 3 hrs. When the reaction was completed, the nanocomposite hydrogel was cut into (3×3 cm) blocks and immersed in repeatedly changed deionized water for 72 hrs to remove the residual monomers. **Tables 5.1-5.2** outline the feed compositions of subsequently prepared hydrogels. Also, the preparation of nanocomposite hydrogel is shown schematically in **Fig 5.1.**

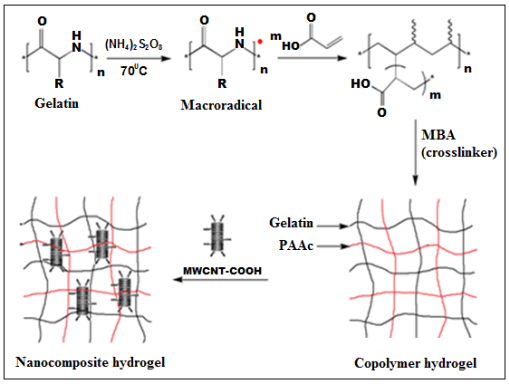

Fig 5.1 Schematic representation for the formation of Gelatin-g-PAAc/MWCNT-COOH nanocomposite hydrogel.

ISSN 2278-2540 | DOI: 10.51583/IJLTEMAS | Volume XV, Issue VI, June 2026

Table 5.1 Recipe in the preparation of Gelatin-g-PAAc/MWCNT-COOH nanocomposite hydrogel with different crosslinker (MBA) content:

Recipe	**GM-1**	**GM-2**	**GM-3**	**GM-4**	**GM-5**
Gelatin (g)	2	2	2	2	2
Acrylic acid (ml)	1.5	1.5	1.5	1.5	1.5
Methylene bis-acrylamide (wt%)	0.05	0.1	0.15	0.2	0.25
Gel fraction determined (%)	54	62	74	82	91
Ionic Conductivity (S/cm $\times 10^{-2}$)	2.50	1.94	1.72	1.58	1.37

*Tetramethylethylene diamine (ml) = 0.05 ml, MWCNT-COOH (wt%) = 0.4 and ammonium persulphate (wt%) = 0.1.

Table 5.2 Recipe in the preparation of Gelatin-g-PAAc/MWCNT-COOH nanocomposite hydrogel with different MWCNT-COOH content:

Recipe	**GA**	**GA-1**	**GA-2**	**GA-3**	**GA-4**	**GA-5**	**GA-6**
Gelatin (g)	2	2	2	2	2	2	2
Acrylic acid (ml)	1.5	1.5	1.5	1.5	1.5	1.5	1.5
MWCNT (wt%)	0	0.1	0.2	0.3	0.4	0.5	0.6
Ionic Conductivity (S/cm $\times 10^{-2}$)	0.92	1.65	2.2	2.85	3.41	3.92	4.52

*Tetramethylethylene diamine (ml) = 0.05ml, methylene bis-acrylamide (wt%) = 0.15 and ammonium persulphate (wt%) = 0.1.

Characterization

Fourier transform infrared spectrometer (FTIR)

To gain insights into the structural information of prepared hydrogels, the IR spectra of the hydrogels were recorded with a Nicolet Impact-410 IR spectrometer (USA) in KBr medium at room temperature in the region 4000–450 cm^{-1}.

Poder X-ray diffraction (XRD)

Powder X-Ray diffraction (XRD) data were collected on a Rigaku Miniflex X-ray diffractometer (Tokyo, Japan) with Cu Kα radiation (λ=0.15418 nm) at 30 kV and 15 mA with a scanning rate of $0.05^o\ s^{-1}$ in a 2θ ranges from 20^o - 80^o.

Morphological Analysis

The surface morphology of the composites was observed using a scanning electron microscope (SEM) (Model- JSM-6390LV, JEOL, Japan). The surface of the sample was platinum coated before SEM analysis. Further morphological analysis was done by Transmission electron microscope (JEM 2100) with an acceleration voltage of 200 kv.

Swelling properties

To measure the degree of swelling the hydrogels, dried samples were placed in buffer media of different pH values at room temperature until the hydrated gels reached a stable weight. The swelling behavior under an applied electric field was determined by applying different electric potentials to the nanocomposite hydrogel

ISSN 2278-2540 | DOI: 10.51583/IJLTEMAS | Volume XV, Issue VI, June 2026

in distilled water. The water absorbed on the surface of the hydrogels was removed using filter paper and the weight noted.

$$\text{Swelling \%} = W_s\text{-}W_{dry}/W_{dry} \times 100 \qquad \textbf{(Eqn. 5.1)}$$

where, W_s is the weight of the hydrogel in swollen state and W_{dry} is that of the hydrogel in dry state.

Gel fraction

The weight ratio of the dried hydrogels in rinsed and unrinsed conditions can be assumed as an index of degree of crosslinking or gel fraction. The pieces of hydrogel samples (3×3 cm) were dried for 6 hrs at 50°C under vacuum. Then the sample (3×3 cm) was immersed into excess of double distilled water for 4 days to rinse away unreacted parts. The gels were dried again at 50°C under vacuum. The gel fraction percentage was calculated by the following equation[39]-

$$\text{Gel fraction \%} = W_f/W_i \times 100 \qquad \textbf{(Eqn. 5.2)}$$

where, W_i = Initial weight before rinse and W_f = Final weight after rinse.

Ionic conductivity

Impedance spectroscopy was used to assess the ionic conductivity by using a two electrode cell and an impedance analyzer (HIOKI IM 3570). The impedance spectrum was measured in the frequency range 100 Hz to 1 MHz with potential amplitude of 10 mV at room temperature. The ionic conductivity was calculated using the following equation-

$$\delta = l/R \times A \qquad \textbf{(Eqn.5.3)}$$

where, δ is the ionic conductivity of the nanocomposite hydrogel ($S.cm^{-1}$), l is the thickness of the film (cm), R is the film resistance (Ω) and A is the surface area of the electrodes (cm^2) prior to the measurement, the hydrogel films (2.5 cm×2.5 cm) were immersed in distilled water at room temperature for 24 hrs and the surface water was gently removed before the film were positioned between the electrodes in the measurement cell.

Blood compatibility by hemolytic activity assay

The hemolytic test was performed following the protocol of Das Purkayastha, M. et al, with slight modification.[40] Briefly, fresh goat blood from a slaughterhouse was collected in a centrifuge tube containing anticoagulant, trisodium citrate (3.2%), and was centrifuged at 2500 rpm for 10 min. The supernatant was discarded, and only the erythrocytes were collected. The erythrocytes were further washed three times with PBS (pH 7.4). A 5% (v/v) suspension of erythrocytes in PBS was prepared; 0.95 ml of this erythrocyte solution was placed in a 1.5 ml centrifuge tube and 0.05 ml of sample (0.5 mg dissolved in 1 ml of 0.5% DMSO) was added to it. The tubes were then incubated for 1 hr at 37°C. Triton X-100 (0.2 %) and PBS were taken as the positive and negative controls, respectively, for comparison. After incubation, the tubes were subjected to centrifugation at 2500 rpm for 10 min. Then, 0.2 ml of the supernatant was added to 96-well plate, and finally absorbance was taken at 570 nm in a UV−visible spectrophotometer (Shimadzu UV-2550 UV–visible spectrophotometer).

Hemolysis % = [(Sample O.D – Negative control O.D)/ (Positive control O.D

– Negative control O.D] X 100 **(Eqn. 5.4)**

Loading of vitamin B_{12}

The method of soaking or equilibration was employed for vitamin B_{12} loading. In this method, the amount of buffer necessary for complete swelling of the nanocomposite hydrogel was determined.[41] Dry hydrogel was placed in the drug solution at a concentration of 0.125 wt%, prepared in the buffer solution of pH 7.0 and left

ISSN 2278-2540 | DOI: 10.51583/IJLTEMAS | Volume XV, Issue VI, June 2026

until all the drug solution was sucked up. Then the completely swollen hydrogel loaded with the vitamin B_{12} was placed in an oven at 30^{o}C for drying overnight.

Drug release experiment under electric field

To investigate the release behavior of vitamin B_{12} under electric stimulus, drug loaded hydrogels were placed in the middle of two carbon electrodes in a desired release medium as shown in the **Fig 5.1.** Then, the amount of drug released into the respective medium was monitored by varying factors such as ionic strength of the release medium and the MWCNT-COOH content in the nanocomposite hydrogel. The pulsatile release of vitamin B_{12} under the applied electric field was also determined by applying pulses of electric current at 5 V, 30 min 'ON' and 30 min 'OFF'.

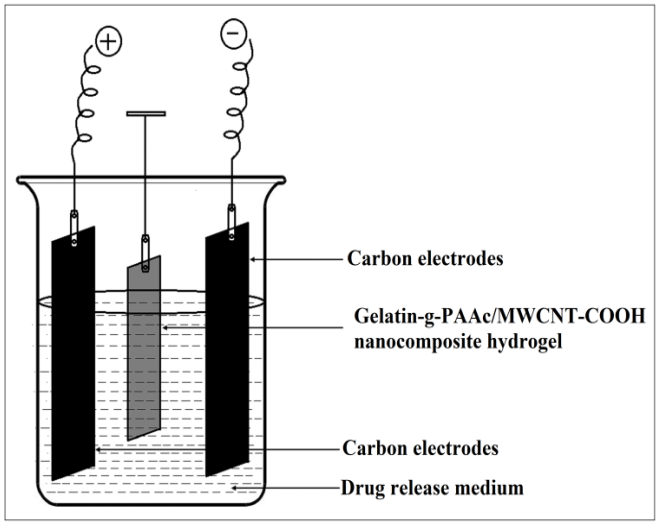

Fig 5.2 Apparatus for electro-responsive drug delivery.

At scheduled time intervals, 5 ml solution was withdrawn and assayed spectrophotometrically by using a UV-visible spectrophotometer (UV-2001Hitachi, Japan) for the determination of the cumulative amount of drug release from the absorbance at 362 nm. To maintain a constant volume, 5 ml of the same solution was returned to the container. The amount of vitamin B_{12} released from the nanocomposite hydrogel was calculated from a calculated from a previously calibrated standard curve.[42]

Experimental Design

Central composite design (face-centered) was used in this study and 2 factors were evaluated, each at 3 levels; experimental trials were performed at all 13 possible combinations to investigate influence of the parameters such as time, MWCNT-COOH content and applied voltage on release behaviour of the drug. Two central composite designs (with electric field and without electric field) were constructed to study the effect of two different factors in each study on drug release behavior. In each case, the two factors, X_1 (time) and X_2 (MWCNT-COOH content); X_1(time) and X_2 (applied voltage) were varied as required by the experimental design and the factor levels were suitably coded **(Table 5.3-5.4)**.

Suppose, we code the levels in standardized units so that the values taken by each of the two variables X_1 and X_2 are -1, 0 and +1.Coded values were obtained by the following formula[43]:

$$Z = (X-X_o)/\Delta X \qquad \textbf{(Eqn. 5.5)}$$

Where, Z is the coded values, X is the corresponding natural value, X_o is the natural value in the center of the domain and ΔX is the increment of X corresponding to one unit of Z.

ISSN 2278-2540 | DOI: 10.51583/IJLTEMAS | Volume XV, Issue VI, June 2026

Table 5.3 Central Composition Design Conditions (without electric field):

Run	**Coded factor levels**	
	X_1	X_2
1	1	1
2	0	1
3	0	0
4	0	0
5	0	0
6	0	0
7	-1	1
8	1	-1
9	0	-1
10	-1	0
11	-1	-1
12	0	0
13	0	0

Translation of coded levels in actual units			
Coded level	**-1**	**0**	**+1**
X_1: Time (hr)	0	5	10
X_2: MWCNT-COOH (wt%)	0.2	0.4	0.6

Table 5.4 Central Composition Design Conditions (with electric field):

Run	**Coded factor levels**	
	X_1	X_2
1	1	0
2	1	-1
3	-1	-1
4	1	1
5	0	1
6	-1	1

ISSN 2278-2540 | DOI: 10.51583/IJLTEMAS | Volume XV, Issue VI, June 2026

7	-1	0
8	0	-1
9	0	0
10	0	0
11	0	0
12	0	0
13	0	0

Translation of coded levels in actual units

Coded level	**-1**	**0**	**+1**
X_1: Time (hr)	0	5	10
X_2: Applied voltage (V)	0	5	10

Again, data were analyzed by multiple regressions to fit the following second order equation:

$$Y = B_o + \sum_{i=1}^{k} B_i X_i + \sum_{i=1}^{k} B_{ij} X_i X_j \qquad \textbf{(Eqn. 5.6)}$$

where, Y = predicted response.

The resulting data were fitted into Design Expert Software (Version 6.0.10 Stat-Ease, USA) and the developed models were adopted for the multiple correlation coefficient (R^2), the adjusted multiple correlation coefficient (adjusted R^2) and corresponding 'P' value provided by analysis of variance (ANOVA). The greater values of R^2 and adjusted R^2 are preferable and it was considered significant when the corresponding 'P' value was less than 0.05. The data were also subjected to 3D response surface methodology to determine the influence of each factor on electro-responsive release behaviour of vitamin B_{12}. Effectiveness of the model is evaluated based on the calculated coefficient of determination (R^2) by the program.

RESULTS AND DISCUSSION

FTIR analysis

FTIR spectra of pristine MWCNT, acid functionalized MWCNT, Gelatin-g-PAAc copolymer and Gelatin-g-PAAc/MWCNT-COOH nanocomposite hydrogels are shown in the **Fig 5.3.** The characteristic bands due to generated polar functional groups on the MWCNT are observed in the FT-IR spectrum of the MWCNTs after chemical oxidation in HNO_3 acid. The FT-IR spectrum of MWCNT–COOH shows absorption peak at 2910 cm^{-1} corresponding to the C-H symmetric stretching vibration. Also, the appearance of peak at 1531 cm^{-1} confirms the existence of carbon double bonding (C=C), which again reveals the integrity of hexagonal structure on the pristine MWCNT.[44] Appearance of peak at 1731 cm^{-1} assigns carbonyl (C=O) stretching vibration of carboxyl groups which is not present in pristine MWCNTs. It confirms the carboxylation on the surfaces of functionalized MWCNTs **(Fig 5.3a).**

ISSN 2278-2540 | DOI: 10.51583/IJLTEMAS | Volume XV, Issue VI, June 2026

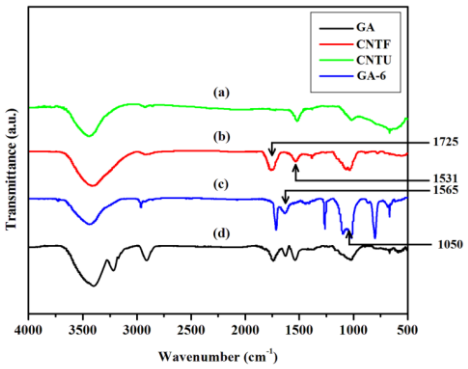

Fig 5.3 FTIR spectra of (a) MWCNT-pristine, (b) MWCNT-COOH, (c) Gelatin-g-PAAc/MWCNT-COOH nanocomposite hydrogels and (d) Gelatin-g-PAAc hydrogel.

FT-IR spectrum of Gelatin-g-PAAc shows absorption peaks at 3391 cm^{-1} and 2950 cm^{-1} which are attributed to the N-H stretching vibration and C-H stretching vibration in $–CH_3$ group. The peaks at 1630 cm^{-1} and 1520 cm^{-1} are due to the amide I (C=O stretching vibration) and amide II (-NH bending vibration) respectively. The absorption peak at 1126 cm^{-1} is due to the C-N stretching vibration of amide III. Also, the characteristic peaks at 3450 cm^{-1}, 1735 cm^{-1} and 613 cm^{-1} are due to the -OH stretching vibration of PAAc, C=O stretching vibration and the -OH out of plane vibration of the carboxylic groups of PAAc, which confirms the grafting reaction. **Fig 5.3c** represents the FT-IR spectrum of Gelatin-g-PAAc/MWCNT-COOH nanocomposite hydrogel which shows characteristics peaks of MWCNT–COOH at 1565 cm^{-1} which is ascribed to the C=C bonding that forms the framework of the carbon nanotube sidewall. The peak at 1050 cm^{-1} indicates the presence of –COOH groups of carboxylated MWCNT and the peaks present in 500-1000 cm^{-1} range indicates the presence of hexagonal carbon atom. Presence of all these characteristics peaks indicates the incorporation of MWCNT–COOH into the Gelatin-g-PAAc hydrogel matrix.

XRD analysis

The diffraction peaks with 2θ values of 25.54º and 45.70º are found for pristine MWCNTs and the diffraction peaks at 26.08º and 43.08º are attributed to the graphite structure (002) and (100) planes of the MWCNT-COOH as shown in the **Fig 5.4**.

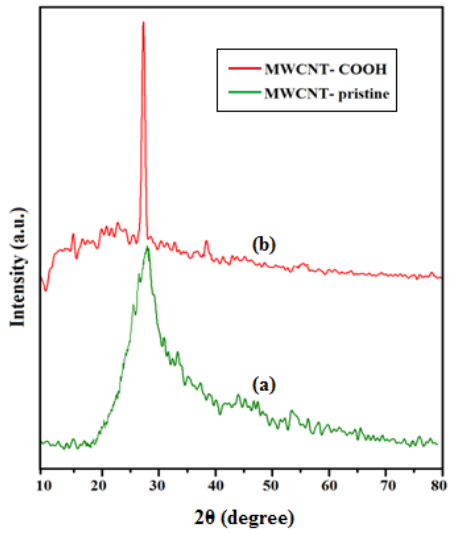

Fig 5.4 XRD patterns of (a) MWCNT-pristine and (b) MWCNT-COOH.

The shifting of characteristic peak position in the XRD pattern of MWCNT-COOH shows the perfect modification of pristine MWCNTs. There is no drastic change in the position of characteristic peaks of pristine MWCNTs and MWCNT-COOH was observed, which suggest that MWCNTs are well retained their original structure even after functionalization.[45]

ISSN 2278-2540 | DOI: 10.51583/IJLTEMAS | Volume XV, Issue VI, June 2026

Fig 5.5 depicts the XRD patterns of Gelatin-g-PAAc copolymer hydrogel and Gelatin-g-PAAc/MWCNT-COOH nanocomposite hydrogels respectively. The XRD pattern of Gelatin-g-PAAc doesn't possess any characteristics peaks, but some minor peaks were observed around 21 and 22°, which could be attributed to minor crystallites of grafted polyacrylic acid chains. On the other hand, the XRD pattern of Gelatin-g-PAAc/MWCNT-COOH shows the characteristics peaks of MWCNT-COOH with low intensity which confirms the incorporation of acid functionalized multiwall carbon nanotubes into the Gelatin-g-PAAc hydrogels.

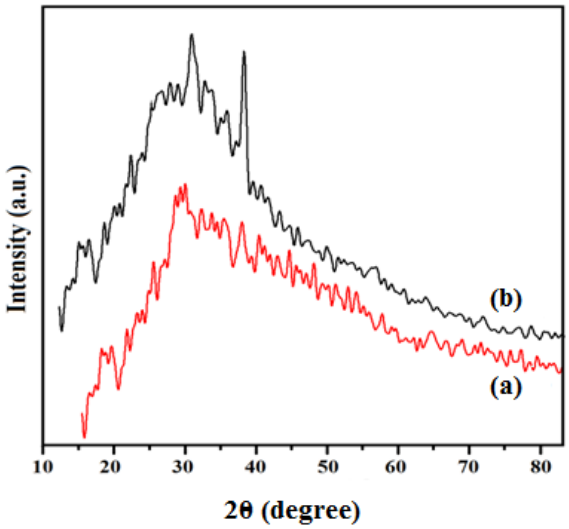

Fig 5.5 XRD patterns of (a) Gelatin-g-PAAc hydrogel and (b) Gelatin-g-PAAc/MWCNT-COOH nanocomposite hydrogels.

Morphological analysis

The morphological images of the copolymer hydrogel and MWCNT-COOH incorporated hydrogels were studied by SEM and are shown in **Fig 5.6.** SEM micrographs indicate the change in the surface morphology of the prepared hydrogels after the incorporation of MWCNT-COOH.

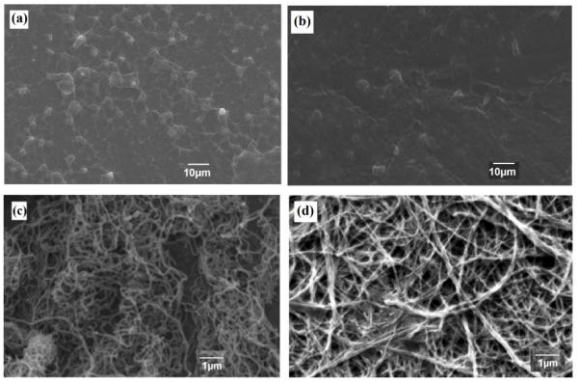

Fig 5.6 SEM images of (a) Gelatin-g-PAAc hydrogel, (b) Gelatin-g-PAAc/MWCNT-COOH nanocomposite hydrogels, (c) MWCNT-pristine and (d) MWCNT-COOH.

A rough surface morphology is observed and some pores can be observed in the micrograph of Gelatin-g-PAAc hydrogel. But, comparatively a smooth surface was observed after the impregnation of MWCNT-COOH into the hydrogel. This observation implies that MWCNT-COOH is uniformly dispersed within the hydrogel. Also, scanning electron microscopy was used to investigate possible MWCNTs fragmentation occurred during treatment. SEM images of MWCNT-COOH and pristine MWCNT are also shown in **Fig 5.6.** From both the micrographs, a significant difference was observed. A sharp surface was observed for the functionalized MWCNT, which was apparently smooth in case of pristine MWCNT. Also, the transparency of nanotubes has been decreased after the functionalization as compared to the pristine MWCNTs which possibly related the introducing of functional groups.[46,47]

ISSN 2278-2540 | DOI: 10.51583/IJLTEMAS | Volume XV, Issue VI, June 2026

Further functionalized MWCNTs morphology characterization was conducted using TEM analysis and **Fig 5.7** represents the TEM micrograph of MWCNT-COOH. No structural damage occurred after acid functionalization of MWCNTs. The MWCNTs retained their original morphology even after the acid treatment.

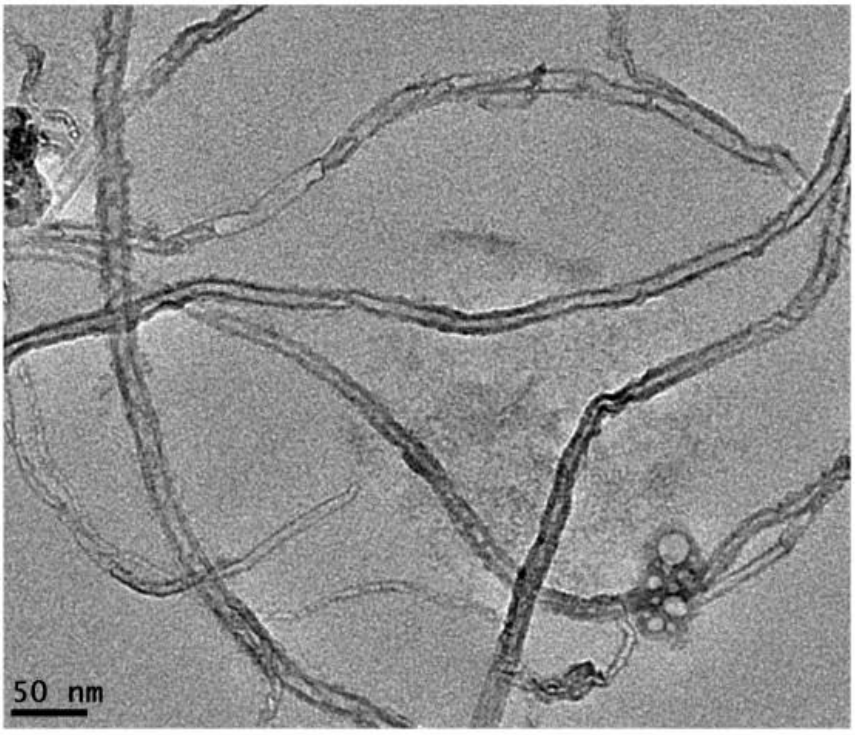

Fig 5.7 TEM image of acid functionalized multiwall carbon nanotubes (MWCNTs).

Ionic Conductivity

Impedance spectroscopy provides a relatively straightforward and rapid technique to assess ionic conductivity. Ionic conductivities of the prepared hydrogels were determined with the variation of crosslinker (MBA) and MWCNT-COOH content in Gelatin-g-PAAc/MWCNT-COOH nanocomposite hydrogel. It was observed that ionic conductivities decrease with an increase in crosslinker (MBA) concentration. It may be due to the decreased proton mobility resulting from increased methylene bis-acrylamide concentration. As the crosslinking density is increased, more crosslinking points will be developed forming a dense network, which will restrict the ionic mobilities of the ionic groups present in the nanocomposite hydrogel. On the other hand, the ionic conductivity was found to be increased with MWCNT-COOH content in the nanocomposite hydrogel. This may be due to the improved ionic transport in presence of MWCNT-COOH in the hydrogel.[48] Ionic conductivities values with the variation of crosslinker and MWCNT-COOH content are given in the **Table 5.1-5.2.**

Swelling study

Effects of pH

The hydrogels have shown tremendous promise in different biomaterial applications because of their unique water holding capacity. Hence, swelling behavior of a particular hydrogel material should be investigated in order to confirm its utility in different biomedical areas. **Fig 5.8** represents the swelling behavior of the prepared nanocomposite hydrogels with different crosslinker amount in acidic (pH=4) and basic (pH=7.4). The swelling behavior was found to be increased with an increase in pH from 4 to 7.4. The gelatin structure is ionizable because the basic dissociation constant (pK_b) of the NH_3^+ is about 6.5 and the acid dissociation constant (pK_a) of the COOH is about 4.7 in gelatin.[49]

ISSN 2278-2540 | DOI: 10.51583/IJLTEMAS | Volume XV, Issue VI, June 2026

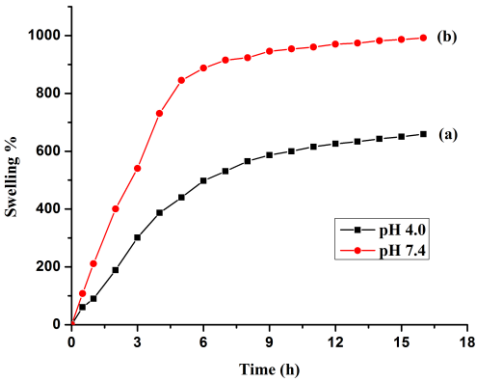

Fig 5.8 Influence of pH of the medium on the swelling behaviours of the nanocomposite hydrogels: (a) pH = 4 and (b) pH = 7.4.

So, this improved swelling behavior is due to the presence of the hydrophilic functional groups (mainly $–COO^-$) in the gelatin structure. Moreover, at higher pH, ionization of the carboxylic acid groups occurs, resulting in electrostatic repulsion between the carboxylate ($–COO^-$) groups as well as expansion of the space network thereby increasing the swelling percentage.[50]

Effect of MWCNT-COOH content

Fig 5.9a depicts the effect of MWCNT-COOH content on the swelling behavior of Gelatin-g-PAAc hydrogels. It was observed that the extent of swelling was decreased with an increase in the concentration of MWCNT-COOH. It may be mainly due to the hydrophobic nature of MWCNT-COOH. The result is consistent with other reports in the literature.[51] Moreover, functionalized MWCNT in Gelatin-g-PAAc may acts as like some crosslinking sites which make the diffusion of water into the hydrogel more difficult. So, interaction between MWCNT-COOH and hydrogels contributed to lower the swelling percentage of the nanocomposite hydrogels than for the native gel.

Effect of applied electric field

The response of an electro-responsive hydrogel in presence of an external electric field depends on the shape and position of the gel between the electrodes.[52] When the gel is placed at a fixed position away from the electrodes, as in our experiment, the swelling behaviour is observed. So, the swelling behavior of the nanocomposite hydrogels with various MWCNT-COOH content were measured as a function of time in distilled water under the applied electric potential of 10V as shown in **Fig 5.9b.**

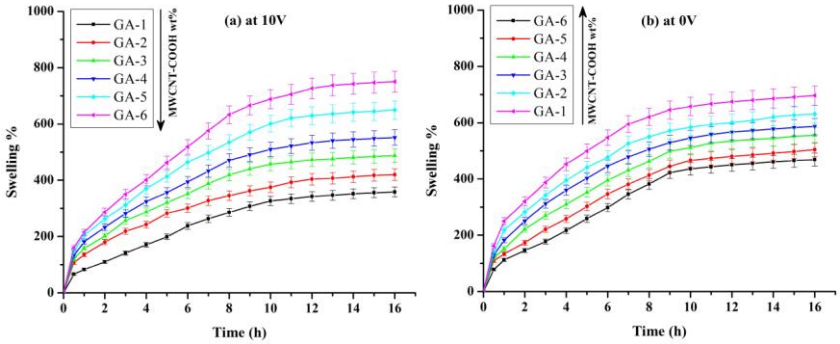

Fig 5.9 Effect of MWCNT-COOH content on the swelling behavior of Gelatin-g-PAAc hydrogels: (a) at 0V and (b) at 10V.

The swelling percentage of Gelatin-g-PAAc/MWCNT-COOH gradually increased with increasing MWCNT-COOH content. MWCNT-COOH provides the efficient pathway of electric field. Therefore, MWCNTs could contribute to the increase in swelling percentage of the nanocomposites by increasing the extent of ionization of the functional groups in the nanocomposite hydrogel under electric voltage applied. This behavior is

ISSN 2278-2540 | DOI: 10.51583/IJLTEMAS | Volume XV, Issue VI, June 2026

completely opposite to the swelling character under normal condition where swelling percentage decreases with increase in MWCNT-COOH content.

Gel fraction

A typical dependency of gel fraction to the quantity of crosslinker incorporated into hydrogels is given in the **Table 5.1**. As seen, the gel fraction of samples is increased by increasing the amounts of crosslinker from 0.05% up to 0.25% by weight. The gel fraction data reveal that the increase in crosslinker amount within the three dimensional network of hydrogel causes an increase in crosslinking density, thus creates more entangled structure.

Blood compatibility studies

Numerous efforts have been given to design novel biomaterials with superior blood compatibility by various research groups. Hemocompatibility is a prime requirement for biomedical applications such as drug delivery, tissue engineering etc. intended for direct or indirect blood exposure. **Fig 5.10** represents the data obtained from hemolysis test as described in Section 5.3.7. The hemolysis test was performed for the nanocomposite hydrogels with 0.1 and 0.6 wt% of MWCNT-COOH content with different concentrations. For all samples, in contact with blood showed a mean hemolysis value less than 0.5 %.The test showed very low hemolysis activity and the data obtained are at the permissible limit as shown in the **Fig 5.10a.** Photographs showing precipitated RBCs at the end of the hemolysis experiment are also given.

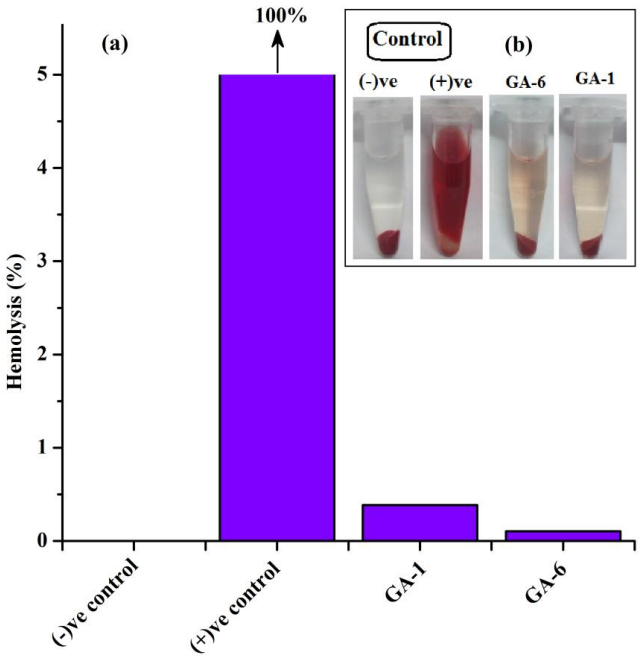

Fig 5.10 Hemolysis results: (a) Hemolysis percentage of the nanocomposite hydrogels with 0.6 wt% (GA-6) and 0.1 wt% (GA-6) MWCNT-COOH content, (b) Photographs of RBCs treated with different samples (GA-6 and GA-1).

Electro-responsive release behavior of vitamin B_{12} from Gelatin-g-PAAc/MWCNT-COOH nanocomposite hydrogels:

Effect of applied voltage

The effect of applied electric potential on release behavior of vitamin B_{12} from Gelatin-g-PAAc/MWCNT-COOH nanocomposite hydrogel is shown in **Fig 5.11.** It can be observed that the drug release rate was much higher under the influence of an electrical stimulus than without electric stimulus. A systematic increase in the drug release rate was observed when the applied voltage was increased from 5 V to 10 V. According to Sawahata et al. drug transport occurs only if the applied electrical current is sufficiently high to induce dimensional changes in the hydrogel. Under higher applied voltage, the ionizable groups are more ionized

ISSN 2278-2540 | DOI: 10.51583/IJLTEMAS | Volume XV, Issue VI, June 2026

which results in improved swelling behavior of the nanocomposite hydrogel. The improved swelling will enhance the release of drug from the nanocomposite hydrogel through diffusion.[53]

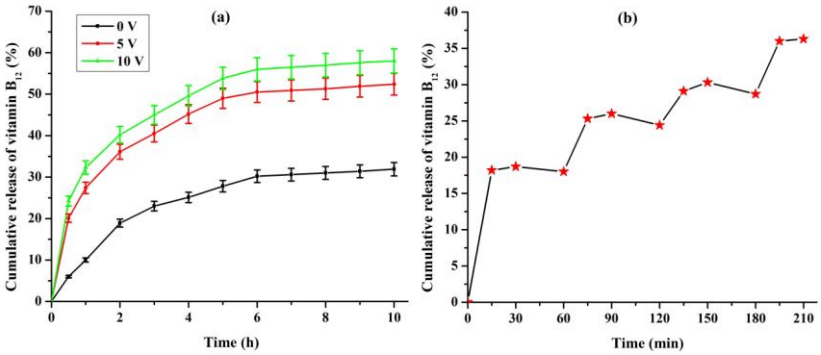

Fig 5.11 Drug release behavior of Gelatin-g-PAAc/MWCNT-COOH nanocomposite hydrogels- (a) At different electric voltage applied: 0 V, 5V and 10 V, (b) Drug release behavior as a function of applied voltage of 0V and 5V, which was altered at 30-min time intervals.

Moreover, the rapid release behaviors of vitamin B_{12} were observed when an electric stimulus was at 'ON' state, whereas they showed a relatively slow release rate during the 'OFF' state while applied electric potential was maintained at 0 and 5V alternately. The plausible reason for this switching pattern of the release of drug molecules is due to the electrically induced changes in osmotic pressure within the gel and local pH gradient attributed to water electrolysis. This could also affect the swelling behaviour of the nanocomposite hydrogel under electric field as well as release of drug from the Gelatin-g-PAAc/MWCNT-COOH nanocomposite hydrogel. In 'OFF' stage (when no electric field), normal diffusion controlled release of drug is taking place which is quite slow.

Effect of ionic strength of the release medium

The ionic strength of the release medium exerts an influence on the release rates of drugs. In our study, the release of vitamin B_{12} was studied in media containing two different ionic strengths, 0.1 M and 0.2 M NaCl solutions. **Fig 5.12** exhibits the release behavior of the drug as a function of ionic strength and at a fixed electric potential of 10 V. It was observed that at higher ionic strengths, the drug release rate was slower with time than in the lower ionic strength media.

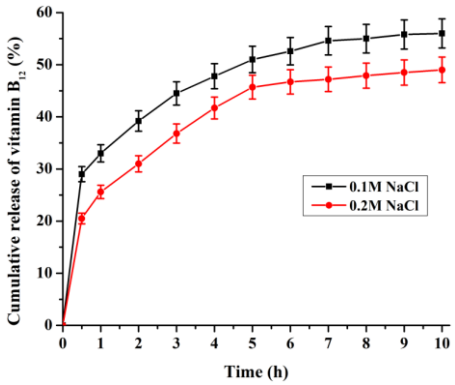

Fig 5.12 Drug release behavior of Gelatin-g-PAAc/MWCNT-COOH nanocomposite hydrogels depending on the ionic strength of the release medium (0.1M and 0.2M NaCl solution).

It may be attributed to the charge screening effect of the additional anions causing a non perfect electrostatic repulsion, which leads to a decreased osmotic pressure difference between the hydrogel network and the external solution. Thereby the shrinkage of the gel was observed instead of swelling. Moreover, the drug solubility may also decrease with increasing ionic strength of the medium, which may also affect in lowering of the drug release rate. Similar behavior was observed by Agnihotri et al. while investigated the electrically modulated release behavior of drug from sodium alginate and carbopol hydrogels. They found that the drug

ISSN 2278-2540 | DOI: 10.51583/IJLTEMAS | Volume XV, Issue VI, June 2026

transport followed the switch-on and switch-off pattern in a pulsatile manner and release rate was significantly decreased with increase in ionic strength of the release medium.[54]

Effect of MWCNT-COOH content

The release of vitamin B_{12} was found to be profoundly dependent on the MWCNT-COOH content of the nanocomposite hydrogels. It can be seen from **Fig 5.13a,** that the drug release rate was decreased as the content of MWCNT-COOH increased when no electric field was applied. On the other hand, a reverse release behavior was observed when an electric potential of 10V was applied to the nanocomposite hydrogels. The release of vitamin B_{12} was found to be increased with increase in MWCNT-COOH content, as predicted from the swelling behavior of nanocomposites in presence of an electric field displayed in **Fig 5.13b.**

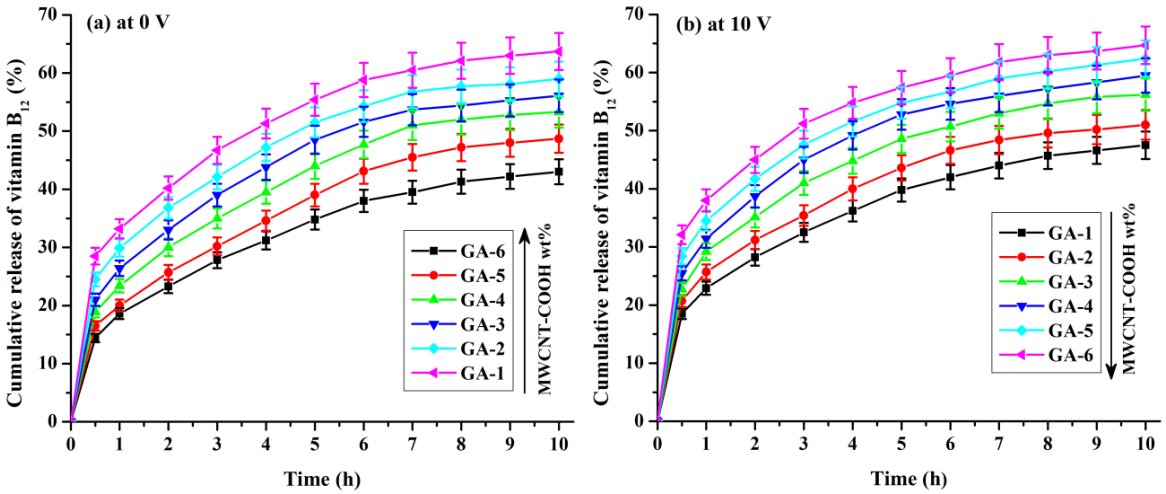

Fig 5.13 Drug release behavior of Gelatin-g-PAAc/MWCNT-COOH nanocomposite hydrogels with various MWCNT-COOH content and at different electric voltage applied: (a) 0 V and (b) 10 V

Response Surface Analysis

The cumulative release % of vitamin B_{12} with respect to two sets of factors was regressed using the Design Expert Software. The multiple regression equation for cumulative drug release % (Y_1) with respect to time (hr) and MWCNT-COOH content:

Final Equation in Terms of Coded Factors

$$\text{Cumulative drug release \% } (Y_1) = 52.25+29.20*X_1+4.58*X_2-22.13*X_1^2-1.38*X_2^2+3.43*X_1*X_2 \quad \textbf{(Eqn. 5.7)}$$

Final Equation in Terms of Actual Factors

$$\text{Cumulative drug release \% } (Y_1) = -6.92011+13.32241*X_1+33.41236*X_2-0.88524*X_1^2-34.52586*X_2^2+3.42500*X_1*X_2 \quad \textbf{(Eqn. 5.8)}$$

The multiple regression equation for cumulative drug release % (Y_2) with respect to time (hr) and applied voltage:

Final Equation in Terms of Coded Factors

$$\text{Cumulative drug release \% } (Y_2) = 49.32+8.35*X_1+20.54*X_2-7.48*X_1^2-14.13*X_2^2+6.53*X_1*X_2 \quad \textbf{(Eqn. 5.9)}$$

Final Equation in Terms of Actual Factors

ISSN 2278-2540 | DOI: 10.51583/IJLTEMAS | Volume XV, Issue VI, June 2026

Cumulative drug release % (Y_2) = -5.34788+3.35723*X_1+8.45369*X_2-0.29915*X_1^2-

0.56515*X_2^2+0.26100*X_1*X_2 **(Eqn. 5.10)**

The results are plotted in **Fig 5.14.** These results show that the electro-responsive release behaviour of the nanocomposite hydrogels was more significantly influenced by the release time and applied voltage than MWCNT-COOH content in the prepared hydrogel. It can be observed from **Table 5.5** that R^2 is high for all responses, which indicates a high degree of correlation between the experimental and predicted responses. In addition, the predicted R^2 value is in good agreement with the adjusted R^2 value, resulting in reliable models.

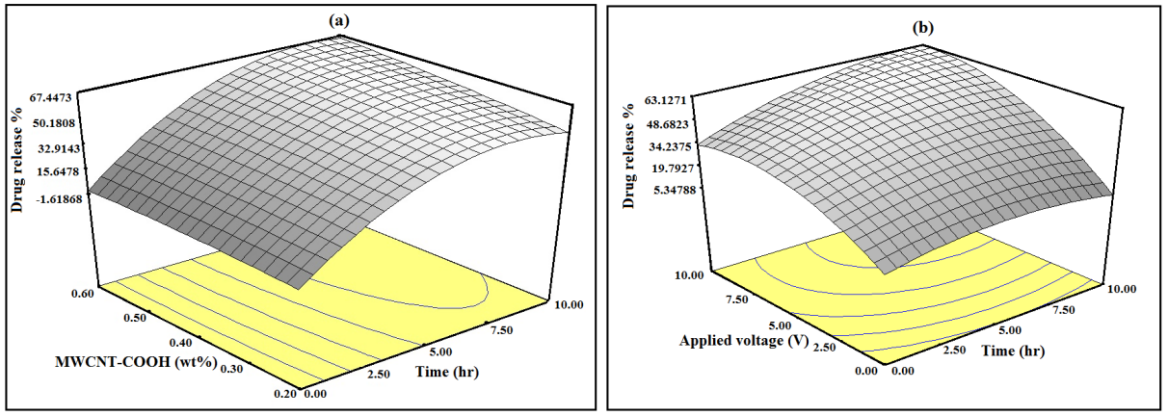

Fig 5.14 3D response surface plot of drug release behaviour of Gelatin-g-PAAc/MWCNT-COOH nanocomposite hydrogel; (a) showing the effect of amount of MWCNT-COOH (wt%) and time (hr) on release behaviour of vitamin B_{12} and (b) showing the effect of applied voltage (V) and time (hr) on release behaviour of vitamin B_{12}.

Table 5.5 Regression statistics table:

Regression Statistics		
	Y_1	Y_2
Predicted-R	0.9742	0.6721
R -square	0.9973	0.9538
Adjusted-R	0.9954	0.9209
Standard deviation	1.64	6.29
Observations	13	13

CONCLUSION

Nanocomposite hydrogels based on gelatin, partially neutralized acrylic acid and acid functionalized multiwall carbon nanotubes (MWCNT-COOH) have been developed. The shifting of characteristic peak position in the XRD pattern of MWCNT-COOH shows the perfect modification of pristine MWCNTs. Also, the characteristics peaks of MWCNT-COOH in the XRD pattern of Gelatin-g-PAAc/MWCNT-COOH confirm the incorporation of acid functionalized multiwall carbon nanotubes into the Gelatin-g-PAAc hydrogels. SEM studies demonstrated the difference in surface morphology of pristine MWCNTs and after the acid functionalization of MWCNTs along with the smooth surface of the nanocomposite hydrogel, which implies the uniform dispersion of MWCNT-COOH within the nanocomposite hydrogel. Swelling percentage was found to be decreased with an increase in MWCNT-COOH content, when no electric field was applied; but reversed swelling behavior was observed when an external electric field (10 V) was applied. In vitro experiments of percentage hemolysis reveal that the prepared nanocomposite hydrogels possess proficient blood compatibility suitable for biomedical applications. The electro-responsive release behavior of vitamin B_{12} exhibited a considerable dependence on ionic strength of the medium, applied voltage and MWCNT-COOH content of the nanocomposite hydrogels.

ISSN 2278-2540 | DOI: 10.51583/IJLTEMAS | Volume XV, Issue VI, June 2026

Drug release behavior was further investigated by response surface methodology and by applying a central composite design. So, the results obtained in this work lead us to the conclusion that Gelatin-g-PAAc/MWCNT-COOH nanocomposite hydrogels can be a promising platform for the development of electro-responsive drug delivery systems.

REFERENCES

1. Lutolf, M.P. & Hubbell, J.A. Nat. Biotechnol. **23** (1), 47-55, 2005.
2. Pratt, A.B., & Weber, F.E. Biotechnol. Bioeng. **86** (1), 27-36, 2004.
3. Nuttelman, C.R., et al. Matrix Biol. **24** (30), 208-218, 2005.
4. Xiang, Y., et al. Eur. Polym. J. **42** (9), 2125-2132, 2006.
5. Risbud, M.V., et al. J. Control. Rel. **68** (1), 23-30, 2000.
6. Anal, A.K., et al. Recent Pat. Endocr. Metab. Immune Drug Discov. **1** (1), 83-90, 2006.
7. Qiu, Y., & Park, K. Adv. Drug. Deliv. Rev. **53** (3), 321-339, 2000.
8. Berner, B., & Dinh, S.M. Electronically Controlled Drug Delivery, CRC Press, Chicago, 1998.
9. Boruah, M., et al. Adv. Polym. Tech. **32 (S1),** E520–E530, 2013.
10. Chen, G., et al. Carbon **42** (4), 753-759, 2004.
11. Boruah, M., et al. Polym. Compos. **35** (1), 27-36, 2014.
12. Chen, G., et al. Polymer **44** (6), 1781-1784, 2003.
13. Yang, S., et al. Carbon **43** (4), 827-834, 2005.
14. Xiao, Y., et al. J. Mater. Chem. **22** (16), 8076-8082, 2012.
15. Lizundia, E., et al. Macromol. Biosci. **12** (7), 870-881, 2012.
16. Dubois, P., & Alexandre, M. Adv. Eng. Mater. **8** (3), 147-154, 2006.
17. Shiga, T. Adv. Polym. Sci. **134,** 131-163, 1997.
18. Teng, X.W., & Yang, H. J. Mater. Chem. **14** (4), 774-779, 2004.
19. O'Connell, M.J., et al. Chem. Phys. Lett. **342** (3-5), 265-271, 2001.
20. Coleman, J.N., et al. Carbon **44** (9), 1624-1652, 2006.
21. Ross-Murphy, S.B. Polymer **33** (12), 2622-2627, 1992.
22. Brodsky, B., & Ramshaw, J.A.M. Matrix. Biol. **15** (8), 545-554, 1997.
23. Kawai, K., et al. Biomaterials **21** (5), 489-499. 2000.
24. Zhao, F., et al. Biomaterials **23** (15), 3227-3234, 2002.
25. Bigi, A., et al. Biomaterials **19** (7-9), 739-744, 1998.
26. Kulkarni, R.V., et al. J. Appl. Polym. Sci. **115** (2), 1180-1188, 2010.
27. Banga, A.K., & Chien, Y.W. Pharm. Res. **10** (5), 697-702, 1993.
28. Kim, S.Y., & Lee, Y.M. J. Appl. Polym. Sci. **74** (7), 1752-1761, 1999.
29. Tanaka, T., et al. Science **218** (4571), 467-469, 1982.
30. Singh, B., et al. Crit. Rev. Ther. Drug Carrier Syst. **22** (1), 27-106, 2005.
31. Singh, B., et al. Crit. Rev. Ther. Drug Carrier Syst. **22** (3), 215-294, 2005.
32. Sauzet, C., et al. Int. J. Pharm. **378** (1), 23-29, 2009.
33. Mutyaba, M.R., et al. Eur. J. Pharm. Sci. **37** (3-4), 434-441, 2009.
34. Leonardi, D., et al. J. Pharm. Biomed. Anal. **48** (3), 802-807, 2008.
35. Li, L., et al. J. Pharm. Sci. **26** (5), 929-937, 2013.
36. Boruah, M., et al. RSC Adv. **4** (83), 43865-43873, 2014.
37. Chen, J., et al. Science **282** (5386), 95-98, 1998.
38. Worsley, K.A., et al. J. Am. Chem. Soc. **131** (50), 18153-18158, 2009.
39. Kokabi, M., et al. Eur. Polym. J. **43** (3), 773-781, 2007.
40. Purkayastha, M.D., et al. J. Agric. Food Chem. **61** (45), 10746-10756, 2013.
41. Bajpai, S.K., et al. Iran. Polym. J. **16** (8), 521-527, 2007.
42. van Dijkhuizen-Radersma, R., et al. Biomaterials **23** (6), 1527-1536, 2002.
43. Kim, B., et al. Macromol. Res. **11** (4), 291-295, 2003.
44. Bhattacharyya, S., et al. Biomacromolecules **9** (2), 505-509, 2008.
45. Neelgund, M.G., & Oki, A. J. Nanosci. Nanotechnol. **11** (4), 3621-3629, 2011.
46. Harris, P.J.F., et al. Carbon nanotubes and related structures: new materials for the twenty-first century, Cambridge University Press, United Kingdom, 1999.

ISSN 2278-2540 | DOI: 10.51583/IJLTEMAS | Volume XV, Issue VI, June 2026

47. Salvetat, J.P. Understanding of carbon nanotubes, Germany: Springer-Verlag Berlin, Heidelberg, 2006.
48. Veerapandian, B., et al. Asian J. Sci. Res. **7** (2), 256-261, 2014.
49. Pourjavadi, A., & Mahdavinia, G.R. Turk. J. Chem. **30** (5), 595-608, 2006.
50. Boruah, M., et al. Polym. Compos. DOI 10.1002/pc.22909, 2014.
51. Pourjavadi, A., & Doulabi, M. Solid State Ionics **257,** 32-37. 2014.
52. Murdan, S. J. Controlled Release **92** (1), 1-17, 2003.
53. Sawahata, K., et al. J. Controlled Release **14** (3), 253-262, 1990.
54. Agnihotri, S.A., et al. J. Appl. Polym. Sci. **96** (2), 301-311, 2005.